RELATIONSHIP BETWEEN LOW-CYCLE-FATIGUE AND CRACK PROPAGATION AT ELEVATED TEMPERATURE IN A P/M NI-BASE SUPERALLOY

T. YOKOMAKU, S. FURUTA and K. IWAI*

Low cycle fatigue and crack propagation tests were conducted at 760℃ on a Ni-base P/M superalloy, AF115, to establish the correlation between defect size, stress/strain range, and fatigue life. By treating defects as cracks or notches, the lower or upper bound of fatigue life can be obtained through a fracture mechanics approach based on the strain energy parameter. The linear damage rule for the partitioned lives based on the fatigue and creep strain energy parameters is applicable for the fatigue life estimation under creep conditions.

INTRODUCTION

P/M superalloys have been a promising high temperature material for use in jet engine components, because the P/M technique enables near-net shaping and gives a homogeneous microstructure of highly alloyed materials. However, small defects, such as inclusions and porosities, are inevitable for P/M materials and these defects significantly affect the fatigue life. Therefore, the influence of defects must be incorporated into the fatigue design of structural components using P/M materials.

The fracture mechanics approach for fatigue life estimation was proposed in recent years (1)(2), which is based on fatigue and creep strain energy parameters. However, there have been few reports showing that this approach is applicable for the materials containing various small defects. In the present study, low cycle fatigue and crack propagation properties at 760 ℃ of a P/M superalloy, AF115, were investigated to establish the relationship

* Mechanical Engineering Research Laboratory, Kobe Steel Ltd.
5-5, Takatsukadai 1-chome, Nishi-ku, Kobe, Japan

between fatigue life, defect size and stress/strain range.

EXPERIMENTAL PROCEDURES

Materials

Normal material. The chemical composition of AF115 (in weight %) was 0.05C-10.9Cr-14.9Co-5.9Mo-3.81Ti-3.71Al-0.81Hf-1.86Nb-0.018B-0.05 Zr-balance Ni. Ar-gas atomized powder was screened to -150 mesh (105 μ m in dia.) and stored in a container filled with Ar gas. The powder was loaded in steel cans, hot outgassed, sealed, and hot isostatically pressed for 3 hours at 1,163℃ and a pressure of 98MPa. The pressings were solution-heat-treated at 1,175℃ for 2 hours and aged at 760℃ for 15 hours. The tensile properties of the material are shown in Table 1.

High-defect material. Powder taken out from the container and exposed to the air for a certain period was used as the high-defect material. In some cases, a few artificial inclusions (Alumina particles ranging from 0.05 to 1mm in diameter) were seeded into the low cycle fatigue specimens.

Table 1. Tensile properties of AF115 at 760℃

Temp. (℃)	Y.S. (MPa)	U.T.S (MPa)	Elong. (%)	R.A. (%)	Young's modulus E (MPa)
760	956	1,057	6.7	10.4	16,500

Low Cycle Fatigue(LCF) and Crack Propagation Test

Smooth specimens 7 mm in diameter were used in LCF tests, and center notched specimens 14mm in width and 4mm in thickness were used in creep and fatigue crack propagation tests. LCF tests were performed at 760 ℃ under the following three waveforms;

i) sine waveform : stress ratio($R\sigma$)= 0.1, frequency(ν)= 2.5Hz
ii) triangular waveform : strain ratio($R\varepsilon$)= 0, $\dot{\varepsilon}$ = 0.4%/sec
iii) trapezoidal waveform : $R\sigma$ = 0.1, tensile hold time = 15min

Crack propagation tests were conducted at 760℃ under a sine waveform ($R\sigma$ = 0.1, ν = 5Hz) and a trapezoidal waveform ($R\sigma$ = -1, tensile hold time = 15min). The fatigue and creep J-integral ranges, $\triangle J_f$ and $\triangle J_c$, in fatigue crack propagation test and the creep J-integral, J^*, in static creep crack propagation tests were evaluated by the following equations using load-COD curves(3)(4):

$$\triangle J_f = \triangle K^2/E + S_F/\{B(W-2a)\} \quad (1)$$

$$\triangle J_c = \{S_c(n_c-1)/(n_c+1)\}/\{2B(W-2a)\} \quad (2)$$

$$J^* = \sigma_{net} \cdot COD \quad (3)$$

where $\triangle K$ is stress intensity range, B and W are specimen thickness and width, a is a half crack length, S_F and S_c are areas of fatigue and creep portion in load-COD curve, n_c is the exponent in the creep equation, $\dot{\varepsilon}_c = k\sigma^{nc}$, and σ_{net} is net stress.

RESULTS

Crack Initiation Site and Defect Characteristics

Scanning electron micrographs of the fractured specimens are shown in Fig. 1. In the normal material, small non-metallic inclusions and gas-porosities were identified at fracture origins. The defect size in the material ranged from 0.02 to 0.03 mm. However, in the high-defect material, prior particle boundaries and large pores were observed at the fracture origin. The relationship between defect size and fatigue life is shown in Fig. 2. The defect size is defined here as the radius of a circle encircling the defect.

Fatigue and Creep-Fatigue Properties

The fatigue lives of normal and high-defect materials are compared in Fig. 3. The high-defect material, whose defect size ranges from 0.1 to 0.3mm, has a fatigue life equal to about 1/3 to 1/100 of that of the normal material. The effect of tensile-hold on fatigue life is shown in Fig. 4. The 15 min tensile-hold decreased the life by more than a factor of 100 of the life under continuous cycling. These results reveal that strict quality control and appropriate creep-fatigue design rules are required for the use of AF115 as structural components.

Crack Propagation Properties

The fatigue and static creep crack propagation rates are shown as a function of $\triangle J_f$ and J^* in Fig. 5, and are expressed as follows:

$$da/dN = C_f \cdot \triangle J_f^{mf} = \begin{cases} 2.24\times 10^{-4}\triangle J_f^{2.85} & (\triangle J_f < 2.1\text{kN/m}) \\ 7.76\times 10^{-4}\triangle J_f^{1.12} & (\triangle J_f \geqq 2.1\text{kN/m}) \end{cases} \quad (4)$$

$$da/dt = C_c \cdot J^* = 8.16\times 10^{-2} J^* \quad (5\text{-}1)$$

or

$$da/dN = C_c \cdot \triangle J_c = 8.16\times 10^{-2}\triangle J_c \quad (5\text{-}2)$$

The crack propagation rate under the tensile-hold fatigue test is compared with the static creep crack propagation rate in Fig. 6. These rates are plotted as a function of $\triangle J_c$, and J^* per cycle. The crack propagation rate under tension-hold fatigue test is a little higher than that under static creep, which means there is a slight interaction between fatigue and creep crack propagation.

DISCUSSION

Fatigue Life Estimation

Crack Analysis. The fatigue life of a smooth specimen can be obtained by considering a defect as a crack and integrating equation (4) from the initial defect size, a_i, to the final crack size, a_f. Equation (4) is available only for $R\sigma = 0$, and is therefore modified as follows:

$$da/dN = C_f \cdot \{(1-R\sigma)^{-0.7}\triangle J_f\}^{mf} \tag{6}$$

The $\triangle J_f$ for the smooth specimen is given by the fatigue strain energy parameter, $\triangle W_f$, as(1)(2)

$$\triangle J_f = F\triangle W_f \cdot a \tag{7}$$

$$\triangle W_f = \triangle\sigma^2/(2E) + g(n_f)\cdot A\triangle\sigma^{nf+1}/(n_f+1) \tag{8}$$

$$g(n_f) = \{(n_f+1)/2\pi\}\cdot\{3.85\, n_f\,(1-1/n_f) + \pi/n_f\} \tag{9}$$

where $F=8/\pi$, $\triangle\sigma$ is stress range, and A and n_f are constants in the cyclic stress-strain relation, $\triangle\varepsilon_p = A\triangle\sigma^{nf}$. Therefore, the fatigue life is obtained by the following equation:

$$N_f = \int_{a_i}^{a_f} \frac{a^{-mf}}{[C_f \cdot F \cdot \{(1-R\sigma)^{-0.7}\triangle W_f\}]^{mf}} da \tag{10}$$

Using the cyclic stress-strain parameters ($A = 3.78\times 10^{-22}$, $n_f = 5.56$) and the crack propagation parameters given in equation (4), the correlation between initial defect size, fatigue life, and stress (or strain) range was calculated and represented by the solid curves in Fig. 2. These curves nealy correspond with the lower bound of the experimental life. The difference between the calculated and the experimental results becomes small in the large strain region, which indicates that the largest portion in low cycle fatigue life is the crack propagation life.

The calculated fatigue life curves for the initial defect sizes of

0.025mm and 0.2mm are shown in Fig. 3. These curves closely agree with the experimental data, so it is concluded that the above approach is appropriate to estimate the low cycle fatigue life of materials with small defects.

Notch Analysis. In the above section, defects were treated as cracks. However, the shapes of actual defects, such as inclusions and porosities, are more like notches than cracks. Therefore, the J-integral solution for the crack propagating from a notch root should be used in this case. Applying the concept of stress intensity analysis for a crack at a circular hole by Dowling(5) to this case, $\triangle J_f$ can be obtained as

$$\begin{aligned} \triangle J_f &= F K_t^2 \triangle W_f \cdot (a - a_i) && (a < a_i + l_m) \\ &= F \triangle W_f \cdot a && (a \geqq a_i + l_m) \end{aligned} \qquad (11)$$

where l_m is a specific distance from notch root, equal to $a_i/(K_t^2-1)$, and K_t is a stress concentration factor for the notch. Applying this relation to equation (6), the fatigue life is obtained as

$$N_f = \int_{l_i}^{l_m} \frac{l^{-mf}}{[C_f \cdot F \cdot K_t \cdot \{(1-R\sigma)^{-0.7} \triangle W_f\}]^{mf}} dl + \int_{a_i+l_m}^{a_f} \frac{a^{-mf}}{[C_f \cdot F \cdot \{(1-R\sigma)^{-0.7} \triangle W_f\}]^{mf}} da \qquad (12)$$

The value l_i is the initial crack length at the front of the notch root, which may be the order of microctructural size, such as the secondary γ' size. Here, 2.5 μm was used for l_i ant K_t is assumed to be 3. The result of this calculation is shown as dotted lines in Fig. 2 and 3. These curves denote nealy the upper bound of experimental life. The difference between the solutions for cracks and notches approaches zero when the notch size decreases to 0.025mm, which is equal to the average defect size of the normal material.

Creep-Fatigue Life Estimation

In the tensile-hold fatigue test, the strain energy parameter per cycle can be partitioned into fatigue and creep components, $\triangle W_f$ and $\triangle W_c$. The $\triangle J_c$ is related with $\triangle W_c$ as

$$\triangle J_c = F \triangle W_c \cdot a \qquad (13)$$

$$\triangle W_c = g(n_c) \cdot B \sigma_H^{n_c+1}/(n_c+1) \qquad (14)$$

where σ_H is hold stress, and B and n_c are constants in creep equation, $\dot{\varepsilon}_c = B\sigma^{n_c}$ ($B=1.46\times10^{-32}$, $n_c=10$). The crack propagation life associated with $\triangle W_c$ was obtained by integrating equation (5-2) as follows;

$$N_c = D_c \triangle W_c \tag{15}$$

$$D_c = \ln(a_f/a_i) / \{C_c \cdot F\} \tag{16}$$

The crack propagation life, N_f, associated with $\triangle W_f$ has already been given as equation (10). By applying the linear damage rule for fatigue and creep crack propagation life, the total life, N, can be obtained as

$$1/N = 1/N_f + 1/N_c \tag{17}$$

As shown in Fig. 4, the estimated life agreed well with the experimental life in the tension-hold fatigue test. It is concluded that the strain energy approach based on fracture mechanics is suitable for creep-fatigue design of high temperature structural components using P/M superalloys.

CONCLUSIONS

1)Non-metallic inclusions, porosities and prior-particle boundaries were the major defects affecting fatigue life of AF115.

2)By treating these defects as either cracks or notches, the lower bound (in the case of a crack) or the upper bound (in the case of a notch) of fatigue life can be be obtained from the fatigue strain energy parameter, $\triangle W_f$.

3)Tensile-hold significantly affects the fatigue life of AF115. The linear damage rule for partitioned lives, based on the fatigue and creep strain energy parameters, $\triangle W_f$ and $\triangle W_c$, is suitable for fatigue life estimation under creep conditions.

REFERENCES

(1) Ohtani, R., Kitamura, T., Nitta, A. and Kuwabara, K., ASTM STP 942, 1988, pp.1163-1180.
(2) Yokomaku, T. and Saori, M., Proc. ICF 7, 1989, pp2651-2658.
(3) Taira, S., Ohtani, R, Kitamura, T and Yamada, Y, J. of Soc. Mat. Sci., Japan, 28-308, 1981, pp. 414-420.
(4) Dowling, N.E., ASTM STP 601, 1976, pp. 19-32.
(5) Dowling, N.E., ASTM STP 677, 1979, pp. 247-273.

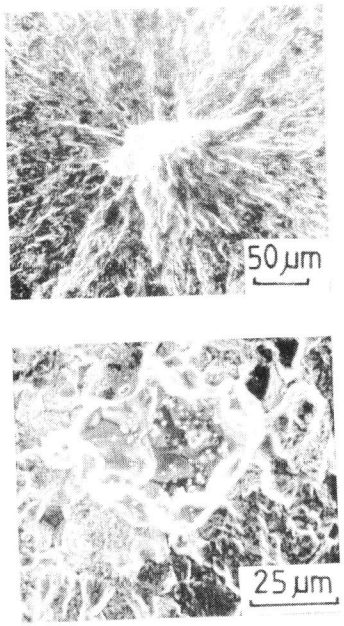

(b)Gas-porosity

Figure 1 Scanning electron micrographs of fracture origin in LCF specimens

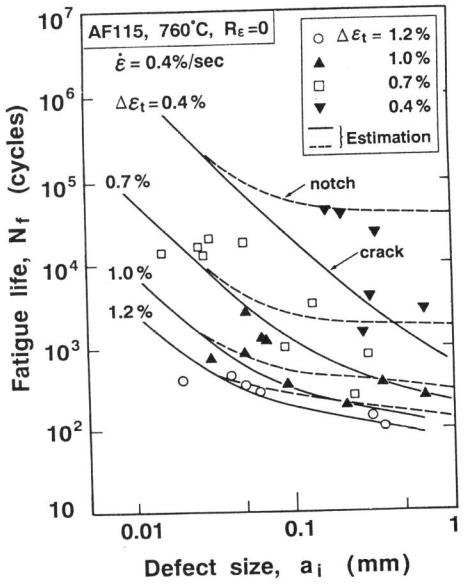

Figure 2 Correlation between defect size and fatigue life

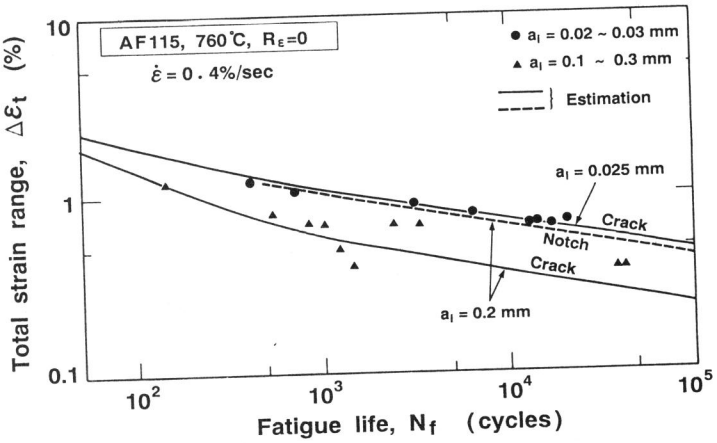

Figure 3 Comparison of LCF life curves of normal and high-defect materials

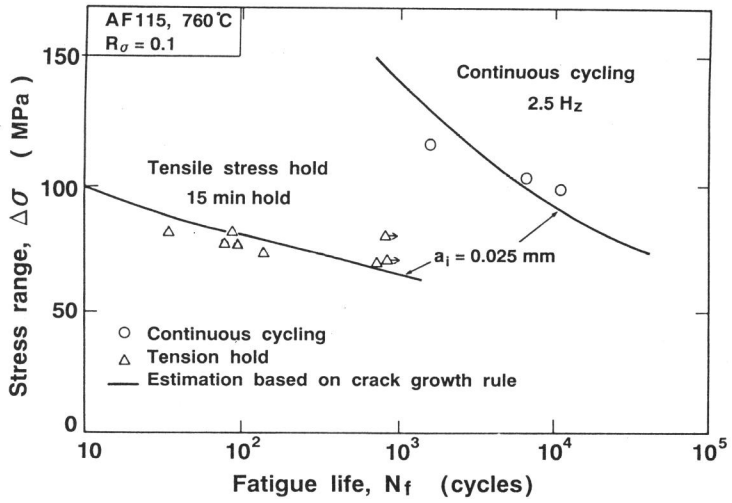

Figure 4 LCF life curves under continuous cycling and tensile-hold waveforms

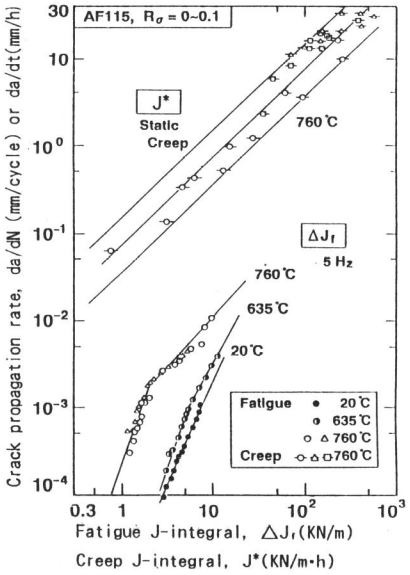

Figure 5 Fatigue and static creep crack propagation rates vs. ΔJ_f and J^*

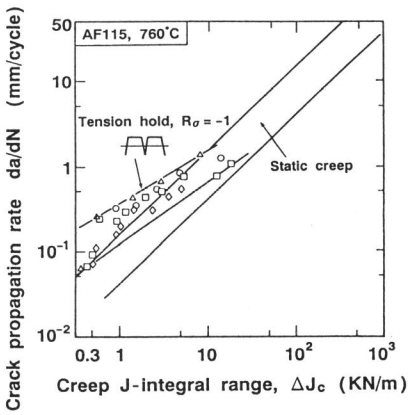

Figure 6 Static creep and creep-fatigue crack propagation rates